Neurobiology of Aging 59 (2017) 41–54

Contents lists available at ScienceDirect

Neurobiology of Aging

journal homepage: www.elsevier.com/locate/neuaging

Klotho regulates postnatal neurogenesis and protects against age-related spatial memory loss

Ann M. Laszczyk, Stephanie Fox-Quick, Hai T. Vo, Dailey Nettles, Phyllis C. Pugh, Linda Overstreet-Wadiche, Gwendalyn D. King*

Department of Neurobiology, University of Alabama at Birmingham, Birmingham, AL, USA

ARTICLE INFO

Article history:
Received 17 January 2017
Received in revised form 22 June 2017
Accepted 21 July 2017
Available online 29 July 2017

Keywords:
Postnatal neurogenesis
Hippocampus
Neural stem cell
Aging
Cognition

ABSTRACT

Although the absence of the age-regulating klotho protein causes klotho-deficient mice to rapidly develop cognitive impairment and increasing klotho enhances hippocampal-dependent memory, the cellular effects of klotho that mediate hippocampal-dependent memory function are unknown. Here, we show premature aging of the klotho-deficient hippocampal neurogenic niche as evidenced by reduced numbers of neural stem cells, decreased proliferation, and impaired maturation of immature neurons. Klotho-deficient neurospheres show reduced proliferation and size that is rescued by supplementation with shed klotho protein. Conversely, 6-month-old klotho-overexpressing mice exhibit increased numbers of neural stem cells, increased proliferation, and more immature neurons with enhanced dendritic arborization. Protection from normal age-related loss of object location memory with klotho overexpression and loss of spatial memory when klotho is reduced by even half suggests direct, local effects of the protein. Together, these data show that klotho is a novel regulator of postnatal neurogenesis affecting neural stem cell proliferation and maturation sufficient to impact hippocampal-dependent spatial memory function.

1. Introduction

Klotho (KL) deficient, knock-out mice (KO) have a shortened life span of ~8 weeks and undergo rapid body-wide deterioration consistent with premature aging (Kuro-o et al., 1997) whereas KL overexpression extends mouse life span (Kuro-o et al., 1997; Kurosu et al., 2005). KL is highly expressed by the kidney where transmembrane KL regulates phosphate homeostasis (Kurosu et al., 2006). Shedding of KL allows it to circulate throughout the body (Imura et al., 2004; Shiraki-Iida et al., 1998) to act as a sialidase (Cha et al., 2008) or an inhibitor of several signaling pathways (Doi et al., 2011; Kurosu et al., 2005; Liu et al., 2007; Zhou et al., 2013). Considerable progress has been made toward understanding the functional relevance of KL in peripheral systems, but very little is known about the specific cellular or molecular actions of KL within the brain.

The brain expresses all forms of KL protein: transmembrane, shed, and secreted (Clinton et al., 2013; Imura et al., 2004; Masso et al., 2015). KL expression is downregulated with age (Duce et al., 2008; King et al., 2012; Yamazaki et al., 2010) and with neurodegenerative disease (Semba et al., 2014) suggesting that KL sensitive pathways and processes are impaired both with normal aging and disease development. Supporting this idea, KO mice rapidly develop cognitive impairment (Nagai et al., 2003) but without gross anatomical abnormalities and only subtly increased apoptosis (Shiozaki et al., 2008) and oxidative stress (Nagai et al., 2003), and decreased synaptic protein expression (Shiozaki et al., 2008). KL-overexpressing mouse (OE) brains have no reported cellular changes although neurons are more resistant to oxidative stress (Brobey et al., 2015; Zeldich et al., 2014). Still, KL overexpression enhances cognitive function concomitant with higher levels of NMDA GluN2B glutamate receptor subunits (Dubal et al., 2014), the subunits known to promote synaptic plasticity (Tang et al., 1999). Overexpression also protects against the development of Alzheimer's disease-like synaptic change and cognitive impairment (Dubal et al., 2015). In humans, a polymorphism that naturally increases the levels of serum KL correlates with increased cognition, suggesting that KL may be important for cognitive reserve (Deary et al., 2005; Dubal et al., 2014; Yokoyama et al., 2015).

* Corresponding author at: Department of Neurobiology, University of Alabama at Birmingham, 1825 University Blvd, Shelby 913, Birmingham, AL 35294, USA. Tel.: 205-996-6247; fax: 205-975-7394.
E-mail address: gdking@uab.edu (G.D. King).

0197-4580/$ – see front matter © 2017 Elsevier Inc. All rights reserved.
http://dx.doi.org/10.1016/j.neurobiolaging.2017.07.008

Since hippocampal immature postnatal-born neurons preferentially express the GluN2B subunit of the NMDA receptor (Ge et al., 2007) and KL-deficiency causes premature aging of peripheral stem cell niches (Liu et al., 2007), herein we assessed the contribution of KL to hippocampal postnatal neurogenesis. We measured the effects of both body-wide, global KL-deficiency and overexpression on neurogenesis at ages before and after onset of cognitive changes as previously reported (Dubal et al., 2014; Nagai et al., 2003). We show that total KL-deficiency causes a premature neurogenic aging-like effect wherein decreased neurogenic capacity begins before the onset of cognitive impairment or peripheral organ system failure. Remarkably, KL overexpression does not affect the niche during early life, but adults show delayed age-related loss of neurogenesis and protection from age-related decline of spatial discrimination. Together these results suggest that KL is a key component of the postnatal stem cell niche and that age-related downregulation of KL expression may contribute to hippocampal decline.

2. Materials and methods

2.1. Animals

Procedures were approved by the UAB IACUC. Global body-wide KL-deficient mice (KO; 129S1/SvImJ) and global body-wide KL-overexpressing mice (OE; C57BL/6J) lines were obtained from M. Kuro-o (University of Texas Southwestern, Dallas, TX, USA), proopiomelanocortin–green fluorescent protein (POMC-GFP) (Overstreet et al., 2004) (C57BL/6J) from L. Overstreet-Wadiche (University of Alabama at Birmingham, Birmingham, AL, USA), and Nestin-GFP (Mignone et al., 2004) (C57BL/6J) from G. Enikolopov (Cold Spring Harbor Laboratory, Cold Spring Harbor, NY, USA). Wild-type (WT; average weight: 3 weeks, 11.6 g; 7 weeks, 20.4 g) and KO (average weight: 3 weeks, 10 g; 7 weeks, 8.1 g) mice were generated by breeding heterozygotes (KL+/−, HET). KO mice die naturally at ~8 weeks of age and thus brains are harvested at or before 7 weeks as detailed. To ensure equivalent KL overexpression, mice carrying the KL overexpression cassette are bred to WT mouse from the same line. Mice were weaned on postnatal day 21. All mice were group housed and had free access to food and water at 26.6 °C with humidity maintained above 40%. KO mice were supplemented with Bacon Softies or Nutra-gel (BioServ, Frenchtown, NJ, USA). As mouse neurogenesis is not gender specific (Lagace et al., 2007), male and female mice were utilized. 5-Bromo-2′-deoxyuridine (BrdU) was intraperitoneally injected (50 mg/kg) either 1x or 4x (2 hours apart), and brains were collected after 30 minutes, 24 hours, 1, 2, or 3 weeks.

2.2. Immunohistochemistry (IHC)

2.2.1. Basic IHC

Tissue was collected after transcardial perfusion with Tyrode's solution (137-mM NaCl, 2.7-mM KCL, 1-mM $MgCl_2$, 1.8-mM $CaCl_2$, 0.2-mM Na_2HPO_4, 12-mM $NaHCO_3$, and 5.5-mM glucose) and 4% paraformaldehyde. Serial 30 μm, free-floating coronal sections representing 1/6th of each brain were permeabilized in Tris-buffered saline containing TritonX-100 (TBST; 50-mM Tris with 0.9% NaCl and 0.5% TritonX-100), incubated with 0.3% H_2O_2, and blocked with 10% horse serum/TBST. When BrdU detection was not required, primary antibodies were incubated in 1% horse serum/TBST for 48 hours. Primary antibodies Ki67 (1:500, anti-rabbit, Abcam Cambridge, MA ab15580), brain lipid-binding protein (BLBP) (1:300, anti-rabbit, EMD Millipore, Billerica, MA ABN14), Dcx (1:50, anti-goat, Santa Cruz Biotechnology, Santa Cruz, CA, sc-8066 or 1:200, anti-rabbit, Abcam ab18723), GFP (green fluorescent protein, 1:100, anti-rabbit, Novus NB600-308), glial fibrillary acidic protein (GFAP, 1:500, anti-rabbit, Dako Z033429), Sox 2 (sex determining region box 2, 1:100, anti-goat, Santa Cruz sc-17320 or anti-rabbit 1:100, R and D Systems), NeuN (1:300, anti-rabbit, Millipore ABN78), neuroD1 (NeuroD1 (ND1); 1:50, anti-goat, Millipore AB15580), or S100β (1:400, anti-rabbit, Dako, Santa Clara CA Z0311) were used. Secondary antibodies conjugated to Alexa 488 or 594 (Life Technologies, Grand Island, NY, USA) were used to detect NeuN, Ki67, and BLBP antibodies. Dcx and Sox2 were detected with biotin conjugated secondary (Southern Biotech, Birmingham, AL, USA) and visualized with streptavidin 488, 594, or 674 (Vector Labs, Burlingame, CA, USA). Nuclei were labeled with 4′,6-diamidino-2-phenylindole (DAPI, Life Technologies) and mounted in Prolong Gold anti-fade mounting media (Life Technologies). ND1 was detected using diaminobenzidine (King et al., 2008, 2011). GFP and GFAP co-localization with KL was detected using 10-μm-thick paraffin sections and anti-KL antibody (R and D Systems, Minneapolis, MN AF1819) as reported (Maltare et al., 2014). This KL antibody is directed against the amino terminus of the KL protein and thus detects all protein forms.

2.2.2. BrdU IHC

After incubating with the co-labeling primary antibody, sections were washed with 2N HCl at room temperature, borate neutralized (0.1-M boric acid, pH 8.5) and incubated with BrdU antibody (1:50, anti-rat, Santa Cruz sc-56258). Biotinylated secondary and streptavidin 594 detected BrdU. Nuclei were labeled with Hoechst (BD Biosciences, San Jose, CA, USA).

2.2.3. Microscopy and quantification

All quantification was performed by genotype-blind researchers. Stereology with optical fractionator software (Stereo Investigator, Version 9, MicroBrightField Inc, Germany) and a Zeiss Axio Imager (Zeiss, Oberkochen, Germany) microscope fitted with a motorized stage and video camera (AxioCam MRc5, Zeiss) (West et al., 1991) was used to estimate subgranular zone (SGZ)–proliferating cells (Ki67 quantifications) every 6th section from −1.34 mm to −2.10 mm from bregma (dissector height: 15 μm with a 5 μm guard zone; fixed counting frame of 80 × 80 μm with a sampling grid size of 75 × 75 μm resulted in 100–200 sites/brain). For all other quantification, images were collected with an Olympus BX53 fluorescent (Center Valley, PA, USA) and the average total number of cells in 3 sections of dorsal hippocampus (1/6th of each brain processed, −1.34 mm to −2.10 mm from bregma) reported (Gilley et al., 2011; Okamoto et al., 2011). Within this same range, maturation stage was defined similar to Plumpe et al. (2006) counting 100 cells unless 3 bregma levels were exceeded first (3 bregma levels counted for 7 weeks KO and 6 months WT). KL dentate co-localization was imaged using confocal Zeiss laser scanning LSM510 microscope (Zeiss, Oberkochen, Germany).

2.2.4. Dendrite analysis

Neuronal morphology of POMC-GFP WT immature neurons was traced from confocal image stacks using Neurolucida, and measurement of total dendrite length was determined by furthest Sholl radius containing measurable dendrite length (v7. MicroBrightField, Williston, VA, USA) (Pugh et al., 2011). Cells with obvious truncation were excluded from analysis.

2.3. Nissl stain

After cresyl violet acetate incubation, slides were dH_2O washed and dehydrated with graded ethanol and xylenes. Volume was estimated in 1/6th of each brain used the Cavalieri estimator and Stereo-Investigator software (−1.22 mm to −3.88 mm from bregma). When dentate was estimated, total volume, dorsal

(−1.22 mm to −2.18 mm from bregma), and ventral (−2.20 to −3.88 mm from bregma) was measured.

2.4. Neurosphere (NSP) assays

2.4.1. Isolation

Progenitors were isolated from 3-week-old hippocampi using 0.05% trypsin. NSPs were grown on non−tissue culture-treated plastics with NeuroCult proliferation media (Stem Cell Technologies, Seattle, WA, USA) containing 10-μg/mL bFGF, (ProSpec, East Brunswick, NJ), 10-μg/mL EGF (ProSpec), and 2-μg/mL heparin (Fisher Scientific). NSPs achieved sufficient confluency for assays ∼2 weeks after isolation, and all assays were completed within 5 passages.

2.4.2. Primary and secondary NSP assays

NSPs were dissociated using Accutase (Fisher Scientific). Reliable survival after plating of 1−5000 cells/well established a minimum of 500 cells/well for viability. 96-well plates received 500 cells/well in complete media with or without 100-ng/mL recombinant mouse KL (R&D Systems). Ten days later, primary NSP number/well and diameter (20−150 μm) were counted. The average/well was reported. Following evaluation, primary NSPs were collected, dissociated, and replated at 500 cells/well. Secondary sphere number and size were evaluated 10 days later. Images of both primary and secondary NSPs were taken with an Evos FL Cell Imaging System, and the diameter of each sphere measured using ImageJ (National Institutes of Health, Bethesda, MD, USA).

2.4.3. Proliferation assay

NSPs were dissociated and plated at 150,000 cells/well on Matrigel (Fisher Scientific) coated coverslips. The next day, half the medium was replaced with 2x 5-ethynyl-2′-deoxyuridine (Fisher Scientific) in complete medium. 5-Ethynyl-2′-deoxyuridine was detected 24 hours later using the manufacturer's Click-iT protocol and IHC as in 1.2 (Logan et al., 2015; Qu et al., 2013; Zeng et al., 2010).

2.5. qPCR

RNA was extracted from flash frozen brain, isolated hippocampi, or NSP cultures using RNA STAT-60 (Tel-Test Inc, Friendswood, TX, USA) and complementary DNA was generated using iScript RT Supermix (Biorad, Hercules, CA, USA) per manufacturer's protocols. Messenger RNA (mRNA) was measured by primer/probe duplex qPCR with SsoFast Probes Supermix (Biorad) and Prime time qPCR assays to the mouse 18s ribosomal subunit (Rn18s: Assay ID Mm.PT.49.3175696.g, IDT, Coralville, IA, USA) and mouse klotho (assay ID Mm.PT.49.11505558; IDT) on a StepOne qPCR system (Applied Biosystems, Foster City, CA). The KL primers will detect both secreted and transmembrane forms of KL. Fold change relative to adult brain was calculated using the ΔΔCt method (Clinton et al., 2013).

2.6. Behavior

2.6.1. Design

Researchers conducting behavior assays were blind to genotype from habituation through scoring. Although the OE mice are physically indistinguishable from WT, the 7-week KO mice are smaller than WT. However, mice are coded to prevent genotypic awareness, and several lines of transgenic mice for other studies were tested concurrently with mice in this study to avoid direct comparison of 7-week-old KO and WT mice. Mice were habituated to the researcher for 3 consecutive days. Groups of mice were processed sequentially through open field, object location, and context-dependent fear conditioning tasks.

2.6.2. Open field

On test day mice were placed in the center of the open field apparatus (43 × 43 × 30 cm plexiglass box). Photo beam detectors quantified all activity for 30 minutes (ENV-515 software, Med Associates, St. Albans, VT, USA).

2.6.3. Object location

Objects of the same height, star shaped plastic bath toys and Lego towers, were mounted on metal washers to prevent tipping. Objects were compared using naïve mice to ensure objects elicited a similar level of exploratory interest. Experimental mice were habituated to a white plexiglass testing chamber (39 × 19 × 21 cm); containing only black tape marking the north facing wall and fresh bedding material for 2 consecutive days. On training day, 2 identical objects were placed on the same side of the box as the black tape and mice were allowed to freely explore for 10 minutes (Haettig et al., 2011). Twenty-four hours later, mice were returned to the box for 5 minutes where 1 object was displaced to the center, back of the box (see Fig. 6E for schematic). Mouse behavior was recorded (TopScan, Clever Sys 2.0, Reston, VA, USA). Videos of task performance were manually scored. Interaction was judged to occur if mice were observed to be facing and sniffing the within 2 cm of a given object. Mice had to explore each object for at least 5 seconds during the training phase and 15 seconds during testing to be included; no mice failed minimum interaction requirements. During training, mice would be excluded if they displayed object/side preference greater than 20%; no mice required exclusion. Percent discrimination was calculated as % of time spent with the moved object−time spent with the non-moved object/total time (Wang et al., 2014).

2.6.4. Context-dependent fear conditioning

Mice were habituated to the testing room for 2 days. On training day, mice were placed in an operant chamber inside an isolation box (Med Associates) for 5 minutes. During that time, mice freely explored for the first 2 minutes. Subsequently, a series of 3, 1 second, 0.5 mA shocks were delivered 1x/minute. Mice remained in the chamber for 2 minutes after the last shock. Twenty-four hours after training, mice were tested by return to the same chamber for 5 minutes. All training and testing was recorded by automated video tracking system (Med Associates). Percent of time spent freezing was manually scored by measuring freezing behavior in 5 seconds intervals.

2.7. Statistics

All data are reported as mean ± standard error of the mean (SEM). Statistical significance is noted if groups differ by p-value less than 0.05 as determined using GraphPad Prism (GraphPad, version 6, La Jolla, CA, USA) using Students t test or 1-way ANOVA as noted in each legend. For qPCR, Dunnett's analysis was conducted to compare each time point to the adult P56. Chi-squar test was performed for 24 hours postinjection BrdU/BLBP and BrdU/S100β due to a low number of cells co-labeling with BrdU.

3. Results

3.1. KL regulates postnatal neurogenesis

Hippocampal development begins around embryonic day 14 and is not complete until the dentate gyrus (dentate) is fully formed ∼2 weeks after birth (Li and Pleasure, 2005, 2014). Thereafter, the dentate SGZ is the only hippocampal neurogenic region. Mouse brain KL expression is first detected during late embryonic development (Takeshita et al., 2004). The

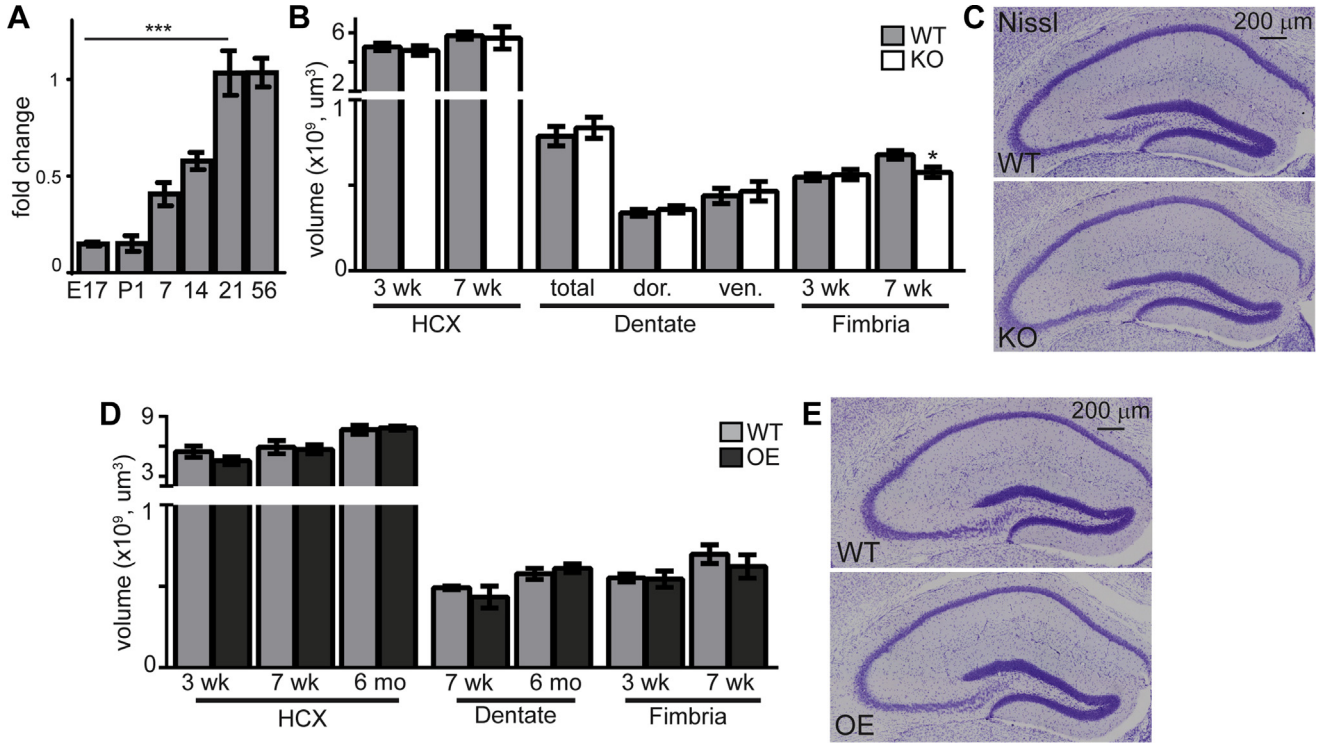

Fig. 1. KL does not affect hippocampal development. (A) Brain KL qPCR fold change after normalization to 18s ribosomal subunit and adult brain KL (P56). KL was detected at embryonic (E) day 17 and postnatal (P) days 1, 7, 14, 21, and 56. (B) Quantification of 3- and 7-week-old WT and KO hippocampus (HCX) and fimbria volume and 7-week dentate gyrus (−1.22 to −3.88 mm from bregma; dor [dorsal: −1.22 to −2.18 mm from bregma], ven [ventral: −2.20 to −3.88 mm from bregma]). (C) Representative 7-week-old WT and KO Nissl stain. Scale bar is 200 μm. (D) Quantification of 3- and 7-week-old WT and OE hippocampus (HCX) and fimbria volume and HCX and dentate volume at 7 weeks and 6 months, as in B. (E) Representative 7-week-old WT and OE Nissl. (n = 6; mean ± standard error of the mean; *t* test: $^{*}p < 0.05$; mRNA: ANOVA, Dunnett's post hoc analysis, $^{***}p < 0.0003$ relative to P56). Abbreviations: ANOVA, analysis of variance; KL, klotho; KO, klotho-deficient knock out mice; mRNA, messenger ribonucleic acid; OE, klotho overexpressing mice; qPCR, quantitative polymerase chain reaction; WT, wild-type.

cerebrospinal fluid generating choroid plexus cells express the highest levels of KL (Kuro-o et al., 1997; Li et al., 2004), but lower level expression is detected in neurons throughout the brain (Clinton et al., 2013; Kuro-o et al., 1997; Li et al., 2017). We measured KL's expression profile during dentate development using mRNA isolated from wild-type (WT) hippocampi embryonic day 17 (E17) to 8 weeks of age. Using a primer/probe set to allow detection of all KL forms, we found that hippocampus achieved adult level KL expression by 3 weeks of age (Fig. 1A), consistent with the reported expression of KL mRNA and protein in mature neurons (Clinton et al., 2013; Li et al., 2017).

KL-deficiency is not reported to disrupt embryonic development. To determine if KL expression affects initial hippocampal or dentate development, we measured hippocampal volume of 3- and 7-week-old WT and KO mice. We confirmed the described fimbria volume decrease in 7-week-old KO mice (Chen et al., 2013) (Fig. 1B). Meanwhile, the volume of the WT and KO hippocampi were indistinguishable at 3 weeks, when initial dentate genesis is complete (Nicola et al., 2015), and at 7 weeks when KO mice are near terminal (Fig. 1B and C). Although KL is overexpressed in the hippocampus of OE mice (Dubal et al., 2014; Li et al., 2017), we found no hippocampal or fimbria volume change at 3 or 7 weeks of age nor were changes detected into adulthood (6 months) (Fig. 1D and E). These data show that gross hippocampal development is not affected by either increasing or decreasing KL protein expression. Herein, the term postnatal neurogenesis is used to distinguish developmental neurogenesis, from ongoing neurogenesis at time points we evaluated on/after postnatal day 21 and selected based on the individual mouse model's life span and cognitive status.

To assess KO and OE postnatal neurogenesis, we measured dorsal hippocampal neurogenic cell populations before and after the onset of reported cognitive change (Dubal et al., 2014; Nagai et al., 2003) (KO at 3 and 7 weeks, white bars throughout; OE at 3 and 6 months, black bars throughout) using strain-relevant WT (gray bars throughout; strain KO:129S1/SvImJ, OE:C57BL/6J) mice to control for strain-specific differences in total neurogenic cell number (Kempermann et al., 1997). At 3 weeks, post-weanling KO mice show no change in the number of stem cells (BLBP), transient amplifying progenitors (TAP: Sox2+/BLBP−), or immature neurons (doublecortin, Dcx) (Fig. 2A–C). However, by 7 weeks, KO mice show a robust loss of stem cells and immature neurons (Fig. 2A–C). In addition, maturation of the immature neurons appears to be reduced, as when their dendritic processes were measured, the percent of cells with a process extending into the granule cell layer was less (Fig. 2D). Meanwhile, although young adult OE mice showed no neurogenic changes at 3 months, all cell populations (stem cells, TAPs, and immature neurons) were increased at 6 months (Fig. 2E–G). Furthermore, there were a greater percentage of immature neurons with a process extending to the granule cell layer suggesting enhanced dendritic maturation (Fig. 2H). Although WT immature neuron total dendrite length was not different between sexes (Supplemental Fig. 1A), to determine if sex was a factor in the KL models, KO and OE cell population counts were separated based on sex. Neither the total number of stem cells nor immature neurons showed sex-specific effects (Supplemental Fig. 1B and C). These data suggest that mouse KL-deficiency causes collapse of the neurogenic niche, but KL overexpression is protective against normal age-related decline of neurogenic capacity.

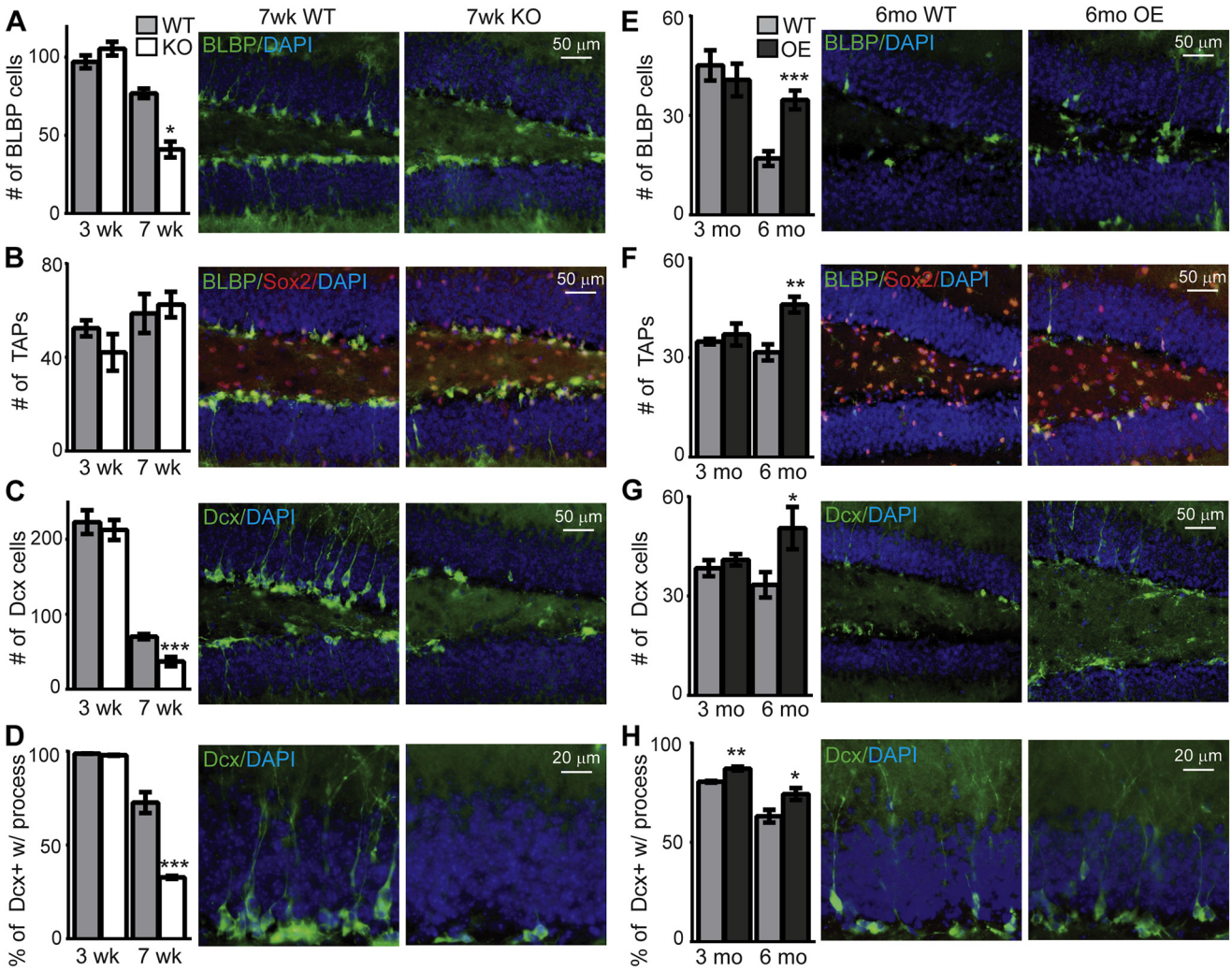

Fig. 2. KL is required for the maintenance of neurogenic cell populations. WT and KO (3 and 7 weeks) or WT and OE (3 and 6 months) neurogenic cell populations are the average total cell number across 3 bregma levels/animal (−1.34 to −2.10 mm) of dorsal hippocampal SGZ. Quantification (graph) and representative images (7 weeks for KO, 6 months for OE) for: (A) and (E) radial-like glial stem cells (brain lipid-binding protein, BLBP; green); (B) and (F) transient amplifying progenitors (TAPs; Sox2+ [red] and BLBP- [green]); and (C) and (G) immature neurons (doublecortin, Dcx; green). Scale bars represents 50 μm. (D) and (H) Immature neuron arborization as the percent of immature neurons with a process extending into the granule cell layer. Scale bar represents 20 μm. DAPI used to label cell nuclei. (n = 3–6 for OE; all others n = 8; mean ± standard error of the mean; *t*-test: $^{*}p < 0.05$, $^{**}p < 0.001$, and $^{***}p < 0.0003$). Abbreviations: KO, klotho-deficient knock out mice; OE, klotho overexpressing mice; SGZ, subgranular zone; WT, wild-type. (For interpretation of the references to color in this figure legend, the reader is referred to the Web version of this article.)

3.2. KL regulates neuronal progenitor proliferation

Outside of the brain, loss of some adult KO stem cell populations is attributed to accelerated stem cell proliferation and premature depletion of the stem cell pool (Liu et al., 2007). We measured the number of SGZ proliferating cells (Ki67+), and at 2 weeks, KO showed no change (Fig. 3A). By 3 weeks, the KO SGZ showed decreased numbers of proliferating cells, the earliest reported KO brain phenotype (Fig. 3A and B). Peripheral stem cells show increased proliferation (Liu et al., 2007), suggesting that KL action on neural progenitors may be unique. Decreased proliferation could result from altered cell cycle dynamics, and as KL is an age-regulating protein, decreased proliferation could be an indicator of premature aging of the neurogenic niche. Although aging does not change cell cycle length (Olariu et al., 2007), it can cause progenitors to re-enter the cell cycle more frequently (Stoll et al., 2011). Thus, we examined KO cell cycle length and re-entry at 3 weeks (Qu et al., 2013) after a single injection of BrdU. As observed with aged stem cells, we measured increased cell cycle re-entry with no cell cycle length change (Fig. 3C). Interestingly, at 7 weeks when fewer stem cells and immature neurons were counted (Fig. 2A and C), more KO SGZ cells are proliferating which may reflect the earlier increased cell cycle re-entry (Fig. 3A). Thus, KL-deficiency affects progenitor cell cycle dynamics causing 3-week KO progenitors to appear phenotypically similar to those in aged brain.

KL modulation of peripheral stem cell proliferation is attributed to the action of circulating KL since peripheral stem cells do not express KL protein (Liu et al., 2007). Since KL is not detected until late embryonic development (Takeshita et al., 2004), it is unlikely that neural stem cells express KL protein. Consistent with previous reports (Clinton et al., 2013; Li et al., 2017), the highest expression of KL is measured in choroid plexus cells, but mature neuronal layers of the hippocampus, including the dentate also express KL protein (Fig. 3E). KL expression is prominent in mature neuronal processes as evidenced by a gradient of increasing KL expression with lowest KL reactivity occurring in SGZ (Fig. 3E). Consistent with low or no SGZ KL expression, confocal microscopy shows no KL co-

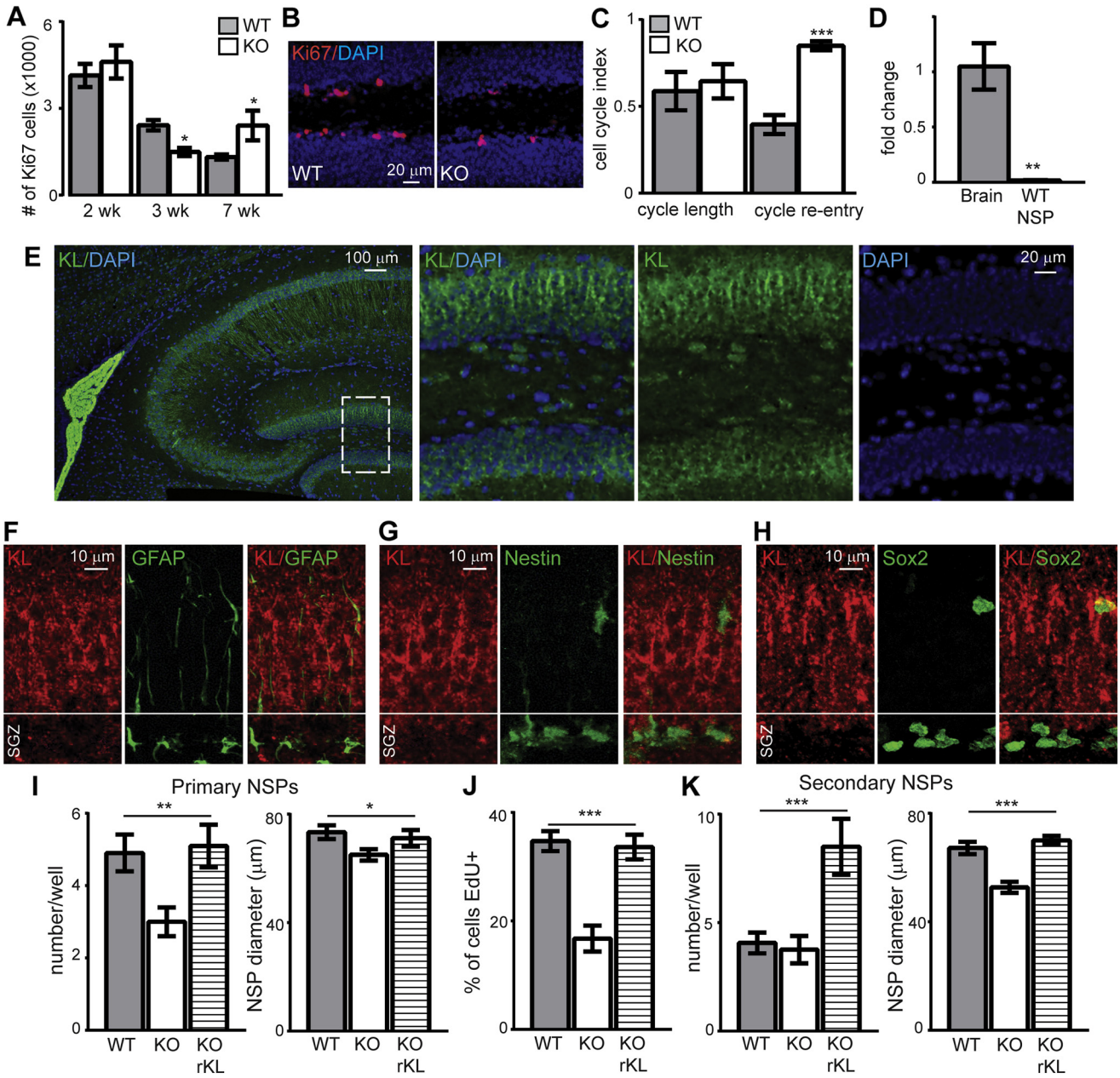

Fig. 3. KL-deficiency reduces proliferation of neurogenic precursors. (A) and (B) WT and KO 2, 3, and 7 weeks stereological quantification and representative 3 weeks IHC of SGZ proliferating cells (Ki67). Cell nuclei labeled with DAPI. Scale bar represents 20 μm. (C) 3-week-old WT and KO mice received 1 BrdU injection to measure cell cycle length ($BrdU^+$+$Ki67^+$/$BrdU^+$) and cell cycle re-entry ($BrdU^+$+$Ki67^+$/$Ki67^+$). (D) Adult hippocampus and 14 days in vitro, primary neurosphere WT qPCR normalized to the 18S ribosomal subunit and adult hippocampus (HCX). (E) Choroid plexus and hippocampal representative WT KL IHC (green) and DAPI (blue) (left) with white dashed box indicating location of higher magnification images (right). Scale bar represents 100 μm or 20 μm. (F) Representative confocal Z stack WT SGZ images of KL (red) and GFAP (green). Nuclei not shown for clarity and scale bar represents 10 μm. (G) Representative confocal Z stacks WT SGZ images of KL (red) and Nestin-GFP (green) from Nestin-GFP WT mice. Nuclei not shown for clarity and scale bar represents 10 μm. (H) Representative confocal Z stacks WT SGZ images of KL (red) and Sox2 (green) from WT mice. Nuclei not shown for clarity and scale bar represents 10 μm. (I) Ten days after plating 500 cells/well, the number and diameter (μm) of WT/KO spheres was measured. Separate wells of KO cells received recombinant mouse KL (rKL) at plating. (J) EdU was added to the media overly laying adherent cells and proliferation measured as the % of cells that were EdU+. (K) Primary spheres (C) were replated as single cells to measure secondary sphere number and diameter (μm) 10 days later. (n = 4–6 in vivo; NSPs: n = 3 independent NSP preparations; F and H are the average of all wells counted ± standard error of the mean, G is the average of 4 fields per coverslip; *t*-test (A, C, and D): $^{**}p < 0.004$, ANOVA (F, G, H, and I): $^{*}p < 0.05$ (multiple comparison test part F, diameter WT vs KO), $^{**}p < 0.005$, and $^{***}p<0.0001$). Abbreviations: ANOVA, analysis of variance; IHC, immunohistochemistry; KL, klotho; KO, klotho-deficient knock out mice; OE, klotho overexpressing mice; qPCR, quantitative polymerase chain reaction; WT, wild-type. (For interpretation of the references to color in this figure legend, the reader is referred to the Web version of this article.)

localization in either Nestin-GFP, Sox2, or GFAP reactive cells most likely to be astrocytes, stem cells, or TAPS when localized to the SGZ (Fig. 3F–H). However, as KL protein expression is lower in hippocampus relative to choroid plexus and KL expressing cells are in close apposition to KL+ SGZ cells, we used qPCR to more specifically measure KL expression by neurogenic precursors. We detected no KL mRNA from stem cells and TAPs isolated from 3-week old mice and cultured as neurospheres (NSP) (Gil-Perotin et al., 2013) (Fig. 3D), further supporting a lack of KL expression in early neural stem cells/progenitors.

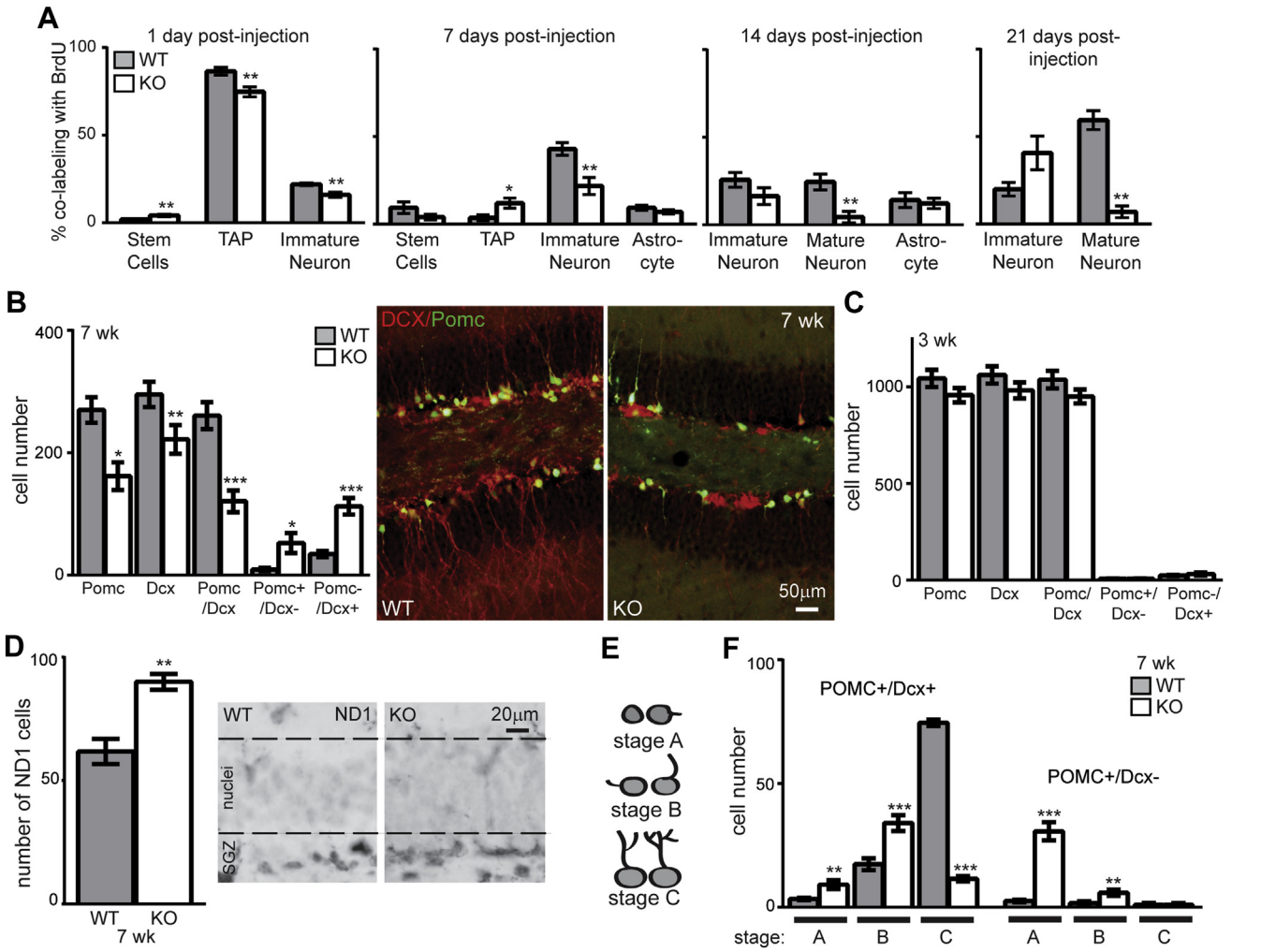

Fig. 4. KL-deficiency impairs neuronal maturation. (A) At 3 weeks of age, WT and KO mice were injected 4x with BrdU. Brains were collected 1, 7, 14, and 21 days postinjection. IHC was performed to detect BrdU co-localization with each neurogenic cell type. The percent of BrdU containing cells that coexpressed each cell-type specific protein was quantified by averaging the total number of cells across 3 bregma levels as above. % of BrdU labeled cells also expressing BLBP (stem cell), Sox2+/BLBP- (TAP), Dcx (immature neuron), S100β (astrocytes), and NeuN (mature neurons). (B) 7 weeks quantification of the total number of POMC+, DCX+, POMC+/DCX+, POMC+/Dcx−, or POMC-/Dcx+ cells in 3 bregma levels and KO/POMC-GFP reporter mouse representative 7-week WT and KO images (Dcx [red] and POMC [green]). DAPI not shown for clarity of neuronal arbors. Scale bars represent 50 μm. (C) Three-week quantification of the total number of POMC+ cells, Dcx+, POMC+/Dcx+, POMC+/Dcx−, or POMC−/Dcx+ cells in 3 bregma levels. (D) 7 weeks representative images and quantification of SGZ cells expressing NeuroD1 (ND1) protein, dashed line added to delineate granule cell layer from SGZ. (E) Morphology scheme used to quantify maturation stage. (F) 7-week quantification of number of POMC+/Dcx+ or POMC+/Dcx- cells by maturation stage. (n = 6 POMC/Dcx, n = 3 for ND1; mean ± standard error of the mean; *t*-test: $^{*}p < 0.05$, $^{**}p < 0.007$, $^{***}p < 0.0004$; chi-square: A stem cells and astrocyte). Abbreviations: IHC, immunohistochemistry; KL, klotho; KO, klotho-deficient knock out mice; OE, klotho overexpressing mice; qPCR, quantitative polymerase chain reaction; WT, wild-type. (For interpretation of the references to color in this figure legend, the reader is referred to the Web version of this article.)

Since neurons are bathed cerebrospinal fluid that contains shed KL (Imura et al., 2004; Kunert et al., 2017; Semba et al., 2014; Shardell et al., 2016; Yamazaki et al., 2010), these data suggest that non-cell autonomous action of shed KL affects early progenitors. Although not taking into account quiescent cells or possible NSP fusion events (Reynolds and Rietze, 2005), primary NSPs estimate the in vivo potential of cells to exhibit stem cell traits (Pastrana et al., 2011). When we plated primary NSPs at the same density, KO NSPs produced fewer, smaller spheres that were less proliferative than WT controls (Fig. 3I and J), confirming our in vivo decreased proliferation (Fig. 3A). If NSPs expressed KL, this would suggest a cell intrinsic mechanism (Gilley et al., 2011); however, our results show that the absence of KL before NSP plating degrades progenitor potential even before major phenotypic differences occur for the mouse. To test if the loss of stem cell potential was permanent, we added recombinant, shed KL to primary KO NSP media and induced rescue of KO NSP size, number, and proliferation (Fig. 3I and J). Using secondary NSPs, we next tested self-renewal. Although secondary KO NSPs self-renewal was not different, forming the same number of spheres as WT, the size of KO spheres was smaller (Fig. 3K). This suggests there is no change in stem:TAP ratio (Piccin and Morshead, 2011) but rather altered cell activity with enhanced KO NSP quiescence. Adding recombinant shed KL rescued size and stimulated greater self-renewal (Fig. 3K). OE mice have broad KL overexpression directed by the human elongation factor 1α promoter (Kurosu et al., 2005). We found that NSPs cultured from OE mice express KL (Supplemental Fig. 2A). However, the expression does not affect baseline measures of the primary NSP number, diameter, or the proliferation of OE spheres, relative to WT (Supplemental Fig. 2B–D). Together these data suggest that KL is a direct and non-cell autonomous regulator of progenitor proliferation and that addition of shed KL can decrease stem cell quiescence.

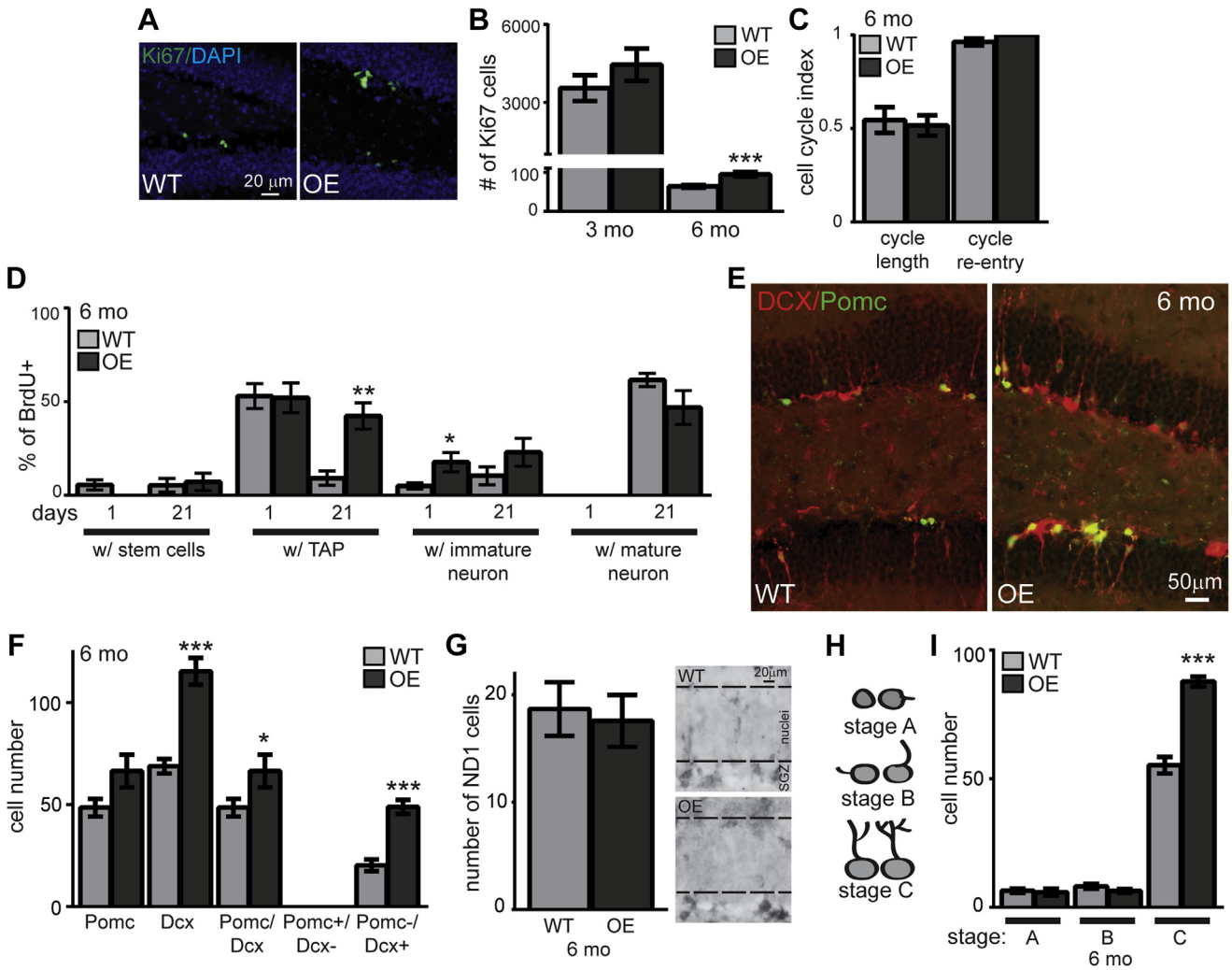

Fig. 5. KL overexpression enhances neuronal maturation. (A) and (B) WT and OE 6-month IHC for proliferating cells (Ki67), 3 and 6 months of stereological quantification. Cell nuclei labeled with DAPI. Scale bar represents 20 μm. (C) 6-month-old mice received 1 BrdU injection to measure cell cycle length ($BrdU^+$+$Ki67^+$/$BrdU^+$) and cell cycle re-entry ($BrdU^+$+$Ki67^+$/$Ki67^+$). (D) 6-month-old WT and OE mice were injected 4x with BrdU. Brains were collected 1 day and 3 weeks (21 days) postinjection. The percent of BrdU cells that co-expressed each cell-type specific protein were quantified as in Fig. 4: stem cells (BLBP+), TAPs (Sox2+/BLBP−), immature neurons (Dcx+), and mature neurons (NeuN+). (E) OE/POMC-GFP reporter mouse representative 6-month WT and OE images (Dcx [red] and POMC [green]). DAPI not shown for clarity of neuronal arbors. Scale bars represent 50 μm. (F) 6-month quantification of the total number of POMC+, Dcx+, POMC+/Dcx+, POMC+/Dcx−, or POMC−/Dcx+ cells. (G) 6-month representative images and quantification of SGZ neuroD1+ cells (ND1) with dashed line added to delineate SGZ from granule cell body layer. (H) Morphology schematic used to quantify maturation stage. (I) 6-months quantification of number of cells POMC+/Dcx+ or POMC+/Dcx-by maturation. (n = 4–6 POMC/Dcx, n = 3 for ND1; mean ± standard error of the mean; *t*-test: $^*p < 0.05$, $^{**}p < 0.007$, and $^{***}p < 0.0004$). Abbreviations: IHC, immunohistochemistry; KL, klotho; KO, klotho-deficient knock out mice; OE, klotho overexpressing mice; WT, wild-type. (For interpretation of the references to color in this figure legend, the reader is referred to the Web version of this article.)

3.3. KL regulates progression of progenitors into mature neurons

KO proliferation is first affected at 3 weeks when short-lived mice (death at ~8 weeks) are young enough to survive assessment of cell fate after proliferation. To track fate, 3-week-old KO mice were injected 4 times with BrdU and were sacrificed 1, 7, 14, or 21 days later. Terminal differentiation to astrocytes (S100β) did not change at any time point (Fig. 4A). As expected, 1 day post-injection WT and KO highly proliferative TAPs (Sox2+/BLBP−) incorporate BrdU more than stem cells (BLBP) (Fig. 4A). KO brains showed fewer co-labeled TAPs as measured by either TAP markers or the earliest expression of Dcx (Fig. 4A, 1 day). As cells matured over the subsequent 3 weeks, the pattern established day 1 continued with fewer immature neurons co-labeling with Dcx at 1 week post-injection and fewer mature neurons labeled with NeuN 2 and 3 weeks post-injection (Fig. 4A). These results show that over the course of neuronal commitment and maturation, the absence of KL causes a failure of progenitors to progress to mature neurons.

To assess maturation dynamics more precisely than allowed by the broad window of Dcx and NeuN expression alone, we bred the KO mouse to POMC-GFP reporter mice wherein dentate neurons that are 1–2 weeks post-mitotic express GFP (Overstreet et al., 2004). We quantified the total number of cells expressing POMC-GFP, Dcx, and co-labeling for both proteins. Dcx is expressed from early neural progenitor commitment through the early integration phases of new neuron maturation (Brown et al., 2003; Rao and Shetty, 2004). POMC expression occurs during a shorter window within the period of Dcx expression (Overstreet et al., 2004) (Fig. 7A). Although 3-week brains showed no change of these immature cell groups, by 7 weeks, all 3 cell groups were decreased in KO mice, consistent with a loss of immature neurons over time (Fig. 4B and C). Whereas 7-week WT brains contain a small number of cells expressing only Dcx (Fig. 4B), in the KO brain the number of

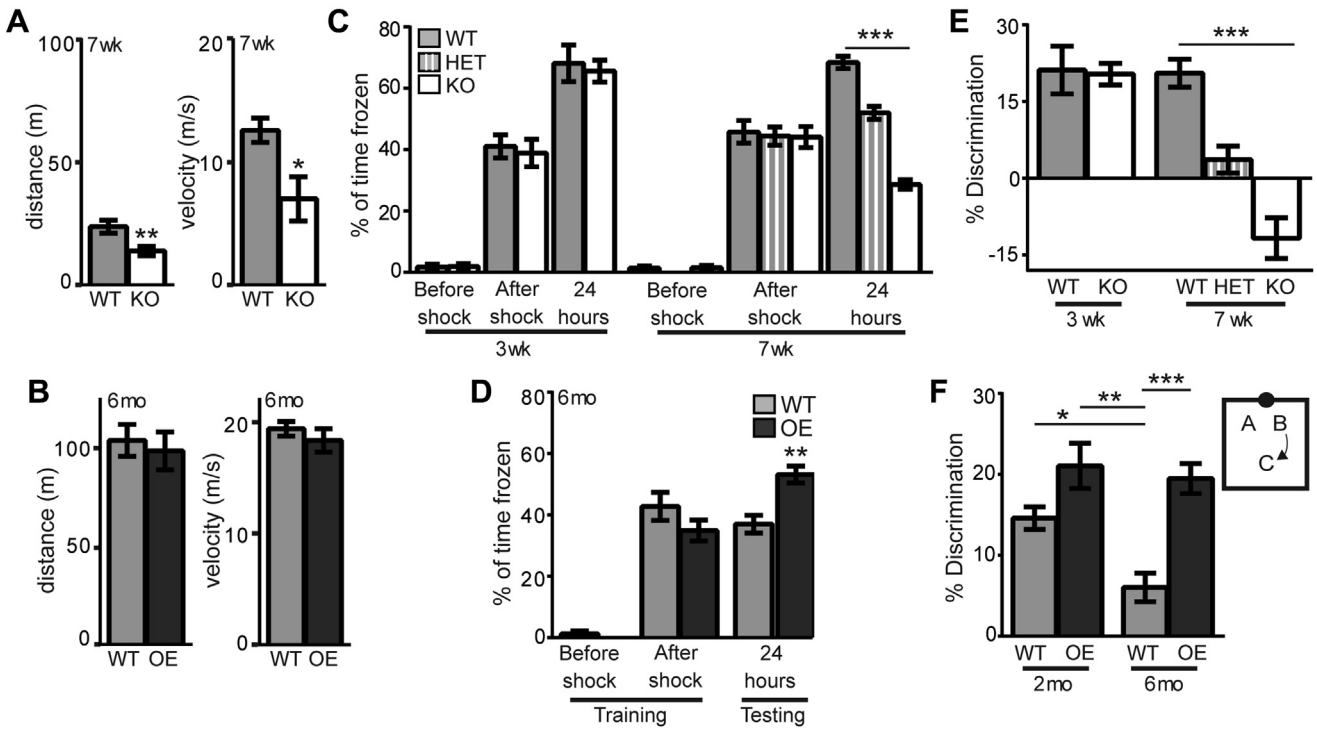

Fig. 6. KL regulates spatial discrimination. (A) 7-week WT and KO open field total distance traveled (meters) and velocity (meters/s). (B) Six-month WT and OE open field as in A. (C) Three-week WT and KO and 7-week WT, HET, and KO context-dependent fear conditioning quantified as % of time spent freezing on training day before and after foot shock and testing day, 24 hours after shock when mice were returned to the same context. (D) Six-month WT and OE context-dependent fear conditioning as in C. (E) Percent discrimination of 3-week WT and KO and 7-week WT, HET, and KO object location. (F) Diagram depicts experimental design of object location task. Quantification of % discrimination of WT and OE mice at age 2 and 6 months. (n = 10–11/genotype; mean ± standard error of the mean; *t* tests A-F, one-way ANOVA C, E; $^{*}p < 0.01$, $^{**}p < 0.004$, and $^{***}p < 0.0001$). Abbreviations: KL, klotho; KO, klotho-deficient knock out mice; OE, klotho overexpressing mice; WT, wild-type.

Dcx only cells increased ~3x and POMC-GFP only cells increased ~5x (Fig. 4B). This suggests an accumulation of immature cells at the earliest stages of neuronal differentiation, an idea we sought to further test by quantifying the number of cells expressing neuroD1 (ND1), a transcription factor required for granule cell differentiation (Gao et al., 2009). Despite the dramatic reduction of Dcx-expressing immature neurons, the number of ND1 expressing cells was increased (Fig. 4D). This could explain why the number of 7-week KO TAPs is not decreased although both stem cells and immature neurons are less numerous (Fig. 2B). Together, these data suggest that the absence of KL not only affects progenitor proliferation but also impairs new neuron maturation at early stages of neuronal commitment.

To further quantify maturation, we classified immature neurons by maturation stage (Plumpe et al., 2006). Stage A cells are adjacent to the SGZ and have no or only a small process extending perpendicular into the granular cell layer. Stage B cells have a process that is beginning to grow toward or into the granule cell layer. Stage C cells are the most mature characterized by processes that extended through the granule cell layer with branching into the molecular layer (Fig. 4E). Most WT POMC+/Dcx+ immature neurons are mature stage C cells but KO immature neurons are stage A and B cells (Fig. 4F). The rare POMC+/Dcx− cells were nearly exclusively all stage A or B cells (Fig. 4F). Decreased KO dendritic complexity (Figs. 2D and 4F) suggests impaired maturation of immature neurons that resembles the phenotype of immature neurons from aged brain (Rao et al., 2005). KL is also important for oligodendrocyte maturation (Chen et al., 2015; Zeldich et al., 2015), suggesting that trophic activity of KL could be required throughout the brain or that different forms of KL protein could have independent effects on different cell populations. Together data from the KO shows that the absence of immature neurons at 7 weeks (Fig. 2A) is the product of progenitors failing to proceed through stages of differentiation and maturation causing suppression of neurogenesis.

The OE neurogenic niche shows several inverse neurogenic phenotypes, although the timing of effects is distinct between the 2 KL models. Previous OE phenotypes are reported only after 4–6 months of age (Dubal et al., 2014, 2015). Likewise, we found OE SGZ showed no proliferation change (Ki67) at 3 months but increased proliferation without an effect on cell cycle by 6 months (Fig. 5A–C). Although neurogenesis is age-downregulated (Ben Abdallah et al., 2010; Rao et al., 2006) and thus very few cells incorporated BrdU at 6 months, we tracked cell fate after proliferation as mentioned previously. Consistent with increased proliferation, the number of BrdU cells co-labeling as TAPs was increased 3 weeks post-injection in the 6-month OE (Fig. 5D). More cells expressing the immature neuron protein Dcx were counted 1 day post-injection with a trend toward more 3 weeks later and with no change in mature neurons (Fig. 5D). Together with the increase in total stem cells, TAPS, and immature neurons (Fig. 2), these results show that KL overexpression enhances proliferation and may affect maturation of adult-born neurons.

To further test whether KL overexpression alters maturation of new neurons, we measured OE/POMC-GFP immature neurons at 3 and 6 months of age. Neither cell number nor maturation stage changed at 3 months (not shown). At 6 months, the number of OE Dcx+ cells was robustly increased (Fig. 5E and F). Unlike the KO, POMC+ only and POMC+/Dcx+ cell groups did not follow the same pattern as Dcx+ alone and were not as robustly increased (Fig. 5F). This could suggest that KL overexpression increases the number of either early and/or late stage immature neurons. To differentiate these possibilities, we quantified cells expressing early neuronal

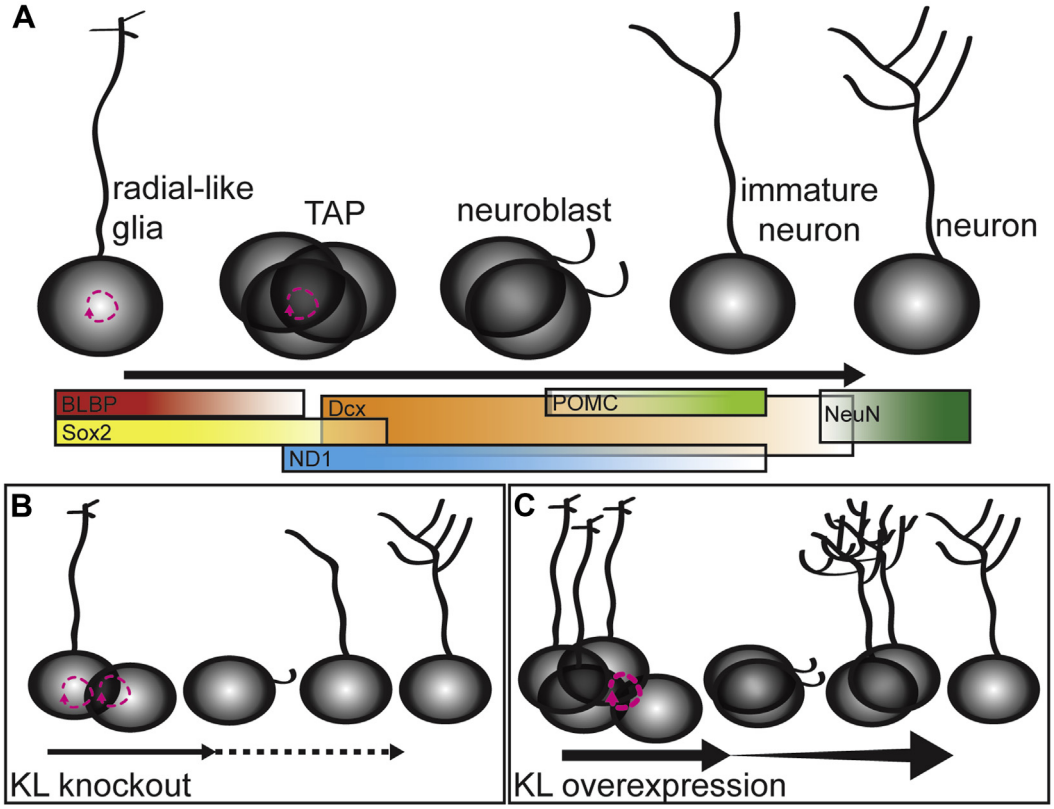

Fig. 7. KL regulates postnatal neurogenesis. (A) Postnatal neurogenesis occurs as stem cells progress through a series of protein expression and morphologic changes to mature into neurons. (B) In brains without KL, with time, there is a loss of the stem/proliferative pool of cells but increased cell cycle re-entry consistent with a prematurely aging neurogenic niche. Decreased proliferation, decreased number of stem cells, and immature neurons were measured, as was delayed maturation of immature neurons. (C) Overexpression of KL increases the number of stem cells/proliferative cells still present at 6 months. Increased proliferation and enhanced maturation allow a greater number of highly arborized immature neurons to persist in the dentate long after normal age-related downregulation of postnatal neurogenesis.

commitment protein ND1 and found no change (Fig. 5G). Rather, maturational staging of Dcx+ cells confirmed an effect on late immature, stage C neurons, with more in the OE (Fig. 5H and I). Thus, although KL overexpression has no effect on cells in young adults, by 6 months, it promotes new neuron generation and enhances dendritic arborization.

3.4. KL regulates spatial memory function

Intact neurogenesis is required for normal dentate function, as selectively manipulating the number of adult born neurons is sufficient to alter the performance of spatial discrimination tasks that have long been associated with dentate gyrus function in pattern separation (Aimone et al., 2014). We thus sought to determine whether KO or OE neurogenic changes are functionally relevant by testing mice on behavioral tasks well established to be affected by altered neurogenesis. We first assessed the mice's motor performance since 7-week-old KO mice are small and kyphotic, in terminal decline (Kuro-o et al., 1997). Open-field assessment showed that 7-week KOs were slower and thus traveled less distance than WT (Fig. 6A). Consistent with previous data (Dubal et al., 2014), 6-month-old OE mice showed no open-field differences (Fig. 6B). But both models are sufficiently mobile to perform behavioral testing at ages when we measure neurogenic changes.

To validate previous reports of hippocampal-dependent memory impairment/enhancement (Dubal et al., 2014; Nagai et al., 2003), we tested context-dependent fear conditioning. During training, all mice froze post-shock (Fig. 6C and D). When returned to the same context 24 hours later, 3-week-old KO mice performed equivalently to WT mice, but 7-week-old KO mice froze less than WT mice (Fig. 6C). As cognitive impairment measured at 7 weeks could be caused by terminal decline of the KO (Kuro-o et al., 1997), we also tested 7-week-old KL-heterozygotic mice (HET) that are physically indistinguishable from WT. KL HET mice show decreased freezing consistent with cognitive impairment 24 hours after training, although impairment was less pronounced than KO mice (Fig. 6C). Although KL heterozygotes do not develop the severe symptoms of loss of KL from renal systems (Kuro-o et al., 1997), they do display lung and heart abnormalities most likely resulting from decreased shed KL (Ishii et al., 2008; Sato et al., 2005; Suga et al., 2000). Meanwhile, consistent with the previous report (Dubal et al., 2014), 6-month OE mice froze more than WT (Fig. 6D). These data confirm the previous reports showing an age-dependent, hippocampal functional role for KL (Dubal et al., 2014; Nagai et al., 2003).

Context-dependent fear conditioning requires the hippocampus and can be affected by selective manipulation of adult neurogenesis but is not an exclusively hippocampal task (Farioli-Vecchioli et al., 2008; Goodman et al., 2010; Ko et al., 2009; Maren et al., 2013; Saxe et al., 2006). To further test hippocampal dentate function, we evaluated object location task performance, which is well established to require the dentate and postnatal neurogenesis (Dees and Kesner, 2013; Goodman et al., 2010; Soule et al., 2008; Wimmer et al., 2012). When mice were free to explore 2 identical objects, they showed no side or object preference on training day but when one of the 2 objects was moved from the north wall, to the center and back of the box (Fig. 6F diagram), 7 but not 3-week-old KO mice explored the

moved object less and may have shown a preference for the nonmoved object (Fig. 6E). Again, loss of even half normal KL level at 7 weeks was sufficient to impair cognitive function of HET mice (Fig. 6E), confirming that poor task performance does not result from systemic decline but rather is specific for KL deficiency. In contrast, 6-month-old OE mice explored the moved object more than WT, consistent with enhanced dentate function (Fig. 6F). Object recognition is stable with increasing mouse age but object location memory diminishes (Wimmer et al., 2012). Increasing circulating KL correlates with increased executive function across human life span (Dubal et al., 2014; Yokoyama et al., 2015). To determine if OE mice showed enhanced discrimination across life span, we also tested the 2-month olds. At 2 months, WT and OE mice performed significantly better than 6-month-old WT mice show no difference relative to 6-month-old OE mice (Fig. 6F). Thus, although WT mouse performance decreased with age, 6-month-old OE mice maintained young-like function (Fig. 6F) at an age when enhanced neurogenesis is also measured (Figs. 2 and 5). Sex-specific spatial memory task performance differences were not detected (Supplemental Fig. 1D and E). Together these data suggest that KL-mediated control of the neurogenic niche is associated with altered function of the dentate, and KL protects against age-related functional decline.

4. Discussion

4.1. KL regulation of adult neurogenesis

Postnatal-born neurons arise from SGZ radial-like glial cells, divide, and proceed through a series of commitment steps where sequential protein expression promotes morphological development into mature granule neurons (Fig. 7A). Here, we show that across shortened life span, KO mice have decreased numbers of stem cells and immature neurons (Figs. 2 and 7B). Decreased proliferation of progenitors and increased cell cycle re-entry are the first detectable alteration and precedes loss of neurogenic cell populations and cognitive impairment (Figs. 2, 3, and 6). KL-deficiency causes delayed TAP/early immature neuron maturation (Fig. 4). Although our data support a non-cell autonomous role for KL on early progenitors (Fig. 3), mature neurons express KL RNA and protein (Clinton et al., 2013; Kuro-o et al., 1997; Li et al., 2017), and it is possible that immature neurons could require KL expression for maturation. Cellular changes to the KO neurogenic niche are consistent with the functional loss of spatial discrimination over life span (Fig. 6) given the prior work showing that altering the number of immature neurons impairs spatial memory (Marin-Burgin and Schinder, 2012). Together, the KO neurogenic niche recapitulates some characteristics of the aged dentate suggesting that KL could be involved in regulating niche aging.

Overexpression of KL induced several inverse effects on neurogenesis. The effect of KL overexpression was not robust until 6 months, consistent with previously observed OE brain phenotypes (Dubal et al., 2014). At this time, KL overexpression protected from age-related loss of spatial discrimination (Fig. 6). Increased spatial discrimination (Fig. 6) occurred at the same time as increased proliferation (Fig. 5), more stem cells, TAPs, and immature neurons (Fig. 2) and enhanced immature neuron maturation (Figs. 5 and 7C). Taken together, these data provide evidence that KL expression level regulates proliferation and maturation of hippocampal neurogenic precursors.

It is important to note that in both model systems, KL is globally manipulated across life span. In the KL-deficient mice, terminal decline of the body could impact brain phenotypes as is observed in human disease (Hermann et al., 2014; Picano et al., 2014). In the KL overexpressing model, overexpression in cells that do not normally make KL could cause nonphysiological effects to be measured. As well in both model systems, all forms of the KL protein are increased or decreased, and it is likely that transmembrane, shed, and secreted forms of KL have unique and even organ-specific mechanisms of action. Even with these considerations noted, however, our results are the first to show inverse effects of KL on a distinct neuronal population that occur at the same time as cognitive effects of the protein begin to be observed. These argue for a direct role of KL within the brain that could be important for healthy brain function. As KL is age-downregulated body-wide (Duce et al., 2008; King et al., 2012) and the polymorphism that increases serum KL correlates with increased cognitive function (Dubal et al., 2014), it is increasingly important to elucidate the cell-type specific functions of KL and determine whether KL could be targeted to support healthy brain aging or as a biomarker of neurodegenerative disease.

4.2. The temporal development of KL brain phenotypes

To date, most KO studies have utilized end of life brains as KO mice have life span of only ~8 weeks. We show that KL reaches adult levels of expression at 3 weeks of age (Fig. 1). At this time, we report reduced neurogenesis and altered stem cell potential (Fig. 3). These data are among the earliest KO reported changes. Other 3-week KO studies found increased serum vitamin D (Tsujikawa et al., 2003; Yoshida et al., 2002), increased skin wnt reporter activation (Liu et al., 2007), and increased lung apoptotic and proliferative indexes (Ishii et al., 2008). Since skin and lung do not express KL (Kuro-o et al., 1997), these data implicate the importance of shed KL. We found that early SGZ progenitors do not express KL but that even when they do, as observed in our cultured OE progenitors, KL expression has no cell autonomous effect (Fig. 3, Supplemental Fig. 2). Rather, the addition of shed KL to cultured progenitor media is sufficient to rescue proliferation defects and promote self-renewal (Fig. 3). Although current genetic models do not allow direct assessment of shed KL under conditions of normal renal, transmembrane KL protein, our results show that isolated NSPs robustly respond to exogenous shed KL. Our data also show that KO line heterozygote mice develop hippocampal-dependent cognitive impairment although half of normal KL is sufficient to maintain renal function, again implicating the importance of shed KL (Ishii et al., 2008; Sato et al., 2005; Suga et al., 2000). Thorough understanding of the direct functions of shed KL is important since targeting a single circulating protein to systemically improve health would be therapeutically useful.

Our data suggest that KL effects are restricted to postnatal neurogenic populations. A pronounced transition occurs between postnatal week 2 and 3 when the hippocampal neurogenic niche takes on the morphologic and protein expression pattern of the adult structure (Nicola et al., 2015), and development-optimized processes are replaced by adult patterns of circuit function (Ben-Ari, 2001). We show steadily increased KL expression that peaks during postnatal week 3 (Fig. 1A), which is also when we measure the first KO cellular phenotypes. These potentially suggest that KL is required for neurogenesis when the brain transitions to adult functionality. We speculate that in the early postnatal environment optimized for neural network formation, redundant mechanisms ensure appropriate neuronal proliferation and maturation even in the absence of KL. However, postnatal and adult brains are less optimized for neurogenesis, and the loss of redundancy reveals a requirement for KL regulation.

It is also intriguing that the neurogenic and cognitive consequences of KL overexpression are not evident until ~6 months of age (Figs. 2, 5, and 6). This could be an effect of the model as OE mice overexpress only ~1.5x normal KL (Kurosu et al., 2005).

However, the cognitive-enhancing human polymorphism, KL-VS, also arises with mild serum KL elevation (Dubal et al., 2014), and minor polymorphic KL changes correlate with human disease risk (Arking et al., 2002, 2005; Deary et al., 2005; Kawano et al., 2002; Tsezou et al., 2008). As such, mild KL increase or decrease may be sufficient to affect brain function especially with increasing age.

4.3. KL function in the brain

The first examination of the OE brain revealed increased expression of hippocampal GluN2B subunits and enhanced dentate LTP (Dubal et al., 2014). GluN2B is the immature NMDA receptor subunit that decreases markedly after birth (Shipton and Paulsen, 2014). Adult born neurons preferentially express GluN2B beginning after commitment to a neuronal fate (Nacher et al., 2007), and these receptors participate in establishment of the first excitatory synapses on adult born neurons (Chancey et al., 2013), underlying enhanced long-term potentiation of immature adult born neurons (Ge et al., 2007). Thus, increased GluN2B and synaptic plasticity reported in the OE dentate could result from enhanced numbers of immature neurons (Figs. 2 and 5). Alternatively, since proliferation and maturation of adult born neurons may be influenced by NMDA receptors, KL-mediated altered expression of GluN2B subunits could contribute to neurogenic changes (Nacher and McEwen, 2006). If increased GluN2B expression is widespread and not restricted to immature neurons, KL-mediated upregulation could impact many forms of hippocampal plasticity.

As knowledge of the role of brain KL increases, it is important to determine which form(s) of the protein mediate cellular and cognitive effects and whether effects are mediated by similar mechanism to those reported peripherally. Until such definition is possible, care must be taken to interpret data where all forms of KL are globally manipulated. The mouse brain is the only organ with all forms of KL protein (Clinton et al., 2013; Imura et al., 2004; Kuro-o et al., 1997; Li et al., 2004; Masso et al., 2015; Shiraki-Iida et al., 1998). Various protein forms, expressed in multiple cell types and circulating in cerebrospinal fluid throughout the brain, provide the potential that KL has widespread actions that likely affect cognition by multiple mechanisms. Our data showing that KL affects dentate neurogenesis with the expected behavioral consequences is likely just one of the mechanisms that contribute to KL's cognitive role. However, as mild life-long overexpression is sufficient to protect against aging-related loss of spatial discrimination and neurogenic aging (Figs. 2 and 6), it is important to determine whether either sustaining KL expression or sustaining expression of specific forms of the protein with age or in old brain protects against age-related cognitive decline.

Disclosure statement

The authors have no conflicts of interest to disclose.

Acknowledgements

The authors would like to thank Drs Irene Masiulis Bowen and Amelia Eisch, University of Texas Southwestern, for advice on BrdU co-labeling protocols; Dr Andrew Kennedy, University of Alabama at Birmingham, for behavioral assay training; and Dr Anita Hjelmeland for use of the Evos Cell Imaging System. Work was funded in part by NIH R00AG034989 and R56AG052936 (GDK) and NIH T32NS061788 (AML).

Appendix A. Supplementary data

Supplementary data associated with this article can be found, in the online version, at http://dx.doi.org/10.1016/j.neurobiolaging.2017.07.008.

References

Aimone, J.B., Li, Y., Lee, S.W., Clemenson, G.D., Deng, W., Gage, F.H., 2014. Regulation and function of adult neurogenesis: from genes to cognition. Physiol. Rev. 94, 991–1026.
Arking, D.E., Atzmon, G., Arking, A., Barzilai, N., Dietz, H.C., 2005. Association between a functional variant of the KLOTHO gene and high-density lipoprotein cholesterol, blood pressure, stroke, and longevity. Circ. Res. 96, 412–418.
Arking, D.E., Krebsova, A., Macek Sr., M., Macek Jr., M., Arking, A., Mian, I.S., Fried, L., Hamosh, A., Dey, S., McIntosh, I., Dietz, H.C., 2002. Association of human aging with a functional variant of klotho. Proc. Natl. Acad. Sci. U. S. A. 99, 856–861.
Ben Abdallah, N.M., Slomianka, L., Vyssotski, A.L., Lipp, H.P., 2010. Early age-related changes in adult hippocampal neurogenesis in C57 mice. Neurobiol. Aging 31, 151–161.
Ben-Ari, Y., 2001. Developing networks play a similar melody. Trends Neurosci. 24, 353–360.
Brobey, R.K., German, D., Sonsalla, P.K., Gurnani, P., Pastor, J., Hsieh, C.C., Papaconstantinou, J., Foster, P.P., Kuro-o, M., Rosenblatt, K.P., 2015. Klotho protects Dopaminergic neuron Oxidant-induced Degeneration by modulating ASK1 and p38 MAPK signaling pathways. PLoS One 10, e0139914.
Brown, J.P., Couillard-Despres, S., Cooper-Kuhn, C.M., Winkler, J., Aigner, L., Kuhn, H.G., 2003. Transient expression of doublecortin during adult neurogenesis. J. Comp. Neurol. 467, 1–10.
Cha, S.K., Ortega, B., Kurosu, H., Rosenblatt, K.P., Kuro-O, M., Huang, C.L., 2008. Removal of sialic acid involving Klotho causes cell-surface retention of TRPV5 channel via binding to galectin-1. Proc. Natl. Acad. Sci. U. S. A. 105, 9805–9810.
Chancey, J.H., Adlaf, E.W., Sapp, M.C., Pugh, P.C., Wadiche, J.I., Overstreet-Wadiche, L.S., 2013. GABA depolarization is required for experience-dependent synapse unsilencing in adult-born neurons. J. Neurosci. 33, 6614–6622.
Chen, C.D., Li, H., Liang, J., Hixson, K., Zeldich, E., Abraham, C.R., 2015. The anti-aging and tumor suppressor protein Klotho enhances differentiation of a human oligodendrocytic hybrid cell line. J. Mol. Neurosci. 55, 76–90.
Chen, C.D., Sloane, J.A., Li, H., Aytan, N., Giannaris, E.L., Zeldich, E., Hinman, J.D., Dedeoglu, A., Rosene, D.L., Bansal, R., Luebke, J.I., Kuro-o, M., Abraham, C.R., 2013. The antiaging protein Klotho enhances oligodendrocyte maturation and myelination of the CNS. J. Neurosci. 33, 1927–1939.
Clinton, S.M., Glover, M.E., Maltare, A., Laszczyk, A.M., Mehi, S.J., Simmons, R.K., King, G.D., 2013. Expression of klotho mRNA and protein in rat brain parenchyma from early postnatal development into adulthood. Brain Res. 1527, 1–14.
Deary, I.J., Harris, S.E., Fox, H.C., Hayward, C., Wright, A.F., Starr, J.M., Whalley, L.J., 2005. KLOTHO genotype and cognitive ability in childhood and old age in the same individuals. Neurosci. Lett. 378, 22–27.
Dees, R.L., Kesner, R.P., 2013. The role of the dorsal dentate gyrus in object and object-context recognition. Neurobiol. Learn. Mem. 106, 112–117.
Doi, S., Zou, Y., Togao, O., Pastor, J.V., John, G.B., Wang, L., Shiizaki, K., Gotschall, R., Schiavi, S., Yorioka, N., Takahashi, M., Boothman, D.A., Kuro-o, M., 2011. Klotho inhibits transforming growth factor-beta1 (TGF-beta1) signaling and suppresses renal fibrosis and cancer metastasis in mice. J. Biol. Chem. 286, 8655–8665.
Dubal, D.B., Yokoyama, J.S., Zhu, L., Broestl, L., Worden, K., Wang, D., Sturm, V.E., Kim, D., Klein, E., Yu, G.Q., Ho, K., Eilertson, K.E., Yu, L., Kuro-o, M., De Jager, P.L., Coppola, G., Small, G.W., Bennett, D.A., Kramer, J.H., Abraham, C.R., Miller, B.L., Mucke, L., 2014. Life extension factor klotho enhances cognition. Cell Rep. 7, 1065–1076.
Dubal, D.B., Zhu, L., Sanchez, P.E., Worden, K., Broestl, L., Johnson, E., Ho, K., Yu, G.Q., Kim, D., Betourne, A., Kuro-O, M., Masliah, E., Abraham, C.R., Mucke, L., 2015. Life extension factor klotho prevents Mortality and enhances cognition in hAPP transgenic mice. J. Neurosci. 35, 2358–2371.
Duce, J.A., Podvin, S., Hollander, W., Kipling, D., Rosene, D.L., Abraham, C.R., 2008. Gene profile analysis implicates Klotho as an important contributor to aging changes in brain white matter of the rhesus monkey. Glia 56, 106–117.
Farioli-Vecchioli, S., Saraulli, D., Costanzi, M., Pacioni, S., Cinà, I., Aceti, M., Micheli, L., Bacci, A., Cestari, V., Tirone, F., 2008. The timing of differentiation of adult hippocampal neurons is crucial for spatial memory. PLoS Biol. 6, e246.
Gao, Z., Ure, K., Ables, J.L., Lagace, D.C., Nave, K.A., Goebbels, S., Eisch, A.J., Hsieh, J., 2009. Neurod1 is essential for the survival and maturation of adult-born neurons. Nat. Neurosci. 12, 1090–1092.
Ge, S., Yang, C.H., Hsu, K.S., Ming, G.L., Song, H., 2007. A critical period for enhanced synaptic plasticity in newly generated neurons of the adult brain. Neuron 54, 559–566.
Gil-Perotin, S., Duran-Moreno, M., Cebrián-Silla, A., Ramírez, M., García-Belda, P., García-Verdugo, J.M., 2013. Adult neural stem cells from the subventricular zone: a review of the neurosphere assay. Anatomical Rec. 296, 1435–1452.
Gilley, J.A., Yang, C.P., Kernie, S.G., 2011. Developmental profiling of postnatal dentate gyrus progenitors provides evidence for dynamic cell-autonomous regulation. Hippocampus 21, 33–47.

Goodman, T., Trouche, S., Massou, I., Verret, L., Zerwas, M., Roullet, P., Rampon, C., 2010. Young hippocampal neurons are critical for recent and remote spatial memory in adult mice. Neuroscience 171, 769–778.
Haettig, J., Stefanko, D.P., Multani, M.L., Figueroa, D.X., McQuown, S.C., Wood, M.A., 2011. HDAC inhibition modulates hippocampus-dependent long-term memory for object location in a CBP-dependent manner. Learn. Mem. 18, 71–79.
Hermann, D.M., Kribben, A., Bruck, H., 2014. Cognitive impairment in chronic kidney disease: clinical findings, risk factors and consequences for patient care. J. Neural Transm. 121, 627–632.
Imura, A., Iwano, A., Tohyama, O., Tsuji, Y., Nozaki, K., Hashimoto, N., Fujimori, T., Nabeshima, Y., 2004. Secreted Klotho protein in sera and CSF: implication for post-translational cleavage in release of Klotho protein from cell membrane. FEBS Lett. 565, 143–147.
Ishii, M., Yamaguchi, Y., Yamamoto, H., Hanaoka, Y., Ouchi, Y., 2008. Airspace enlargement with airway cell apoptosis in klotho mice: a model of aging lung. J. Gerontol. Ser. A Biol. Sci. Med. Sci. 63, 1289–1298.
Kawano, K., Ogata, N., Chiano, M., Molloy, H., Kleyn, P., Spector, T.D., Uchida, M., Hosoi, T., Suzuki, T., Orimo, H., Inoue, S., Nabeshima, Y., Nakamura, K., Kuro-o, M., Kawaguchi, H., 2002. Klotho gene polymorphisms associated with bone density of aged postmenopausal women. J. Bone Miner. Res. 17, 1744–1751.
Kempermann, G., Kuhn, H.G., Gage, F.H., 1997. Genetic influence on neurogenesis in the dentate gyrus of adult mice. Proc. Natl. Acad. Sci. U. S. A. 94, 10409–10414.
King, G.D., Kroeger, K.M., Bresee, C.J., Candolfi, M., Liu, C., Manalo, C.M., Muhammad, A.K., Pechnick, R.N., Lowenstein, P.R., Castro, M.G., 2008. Flt3L in combination with HSV1-TK-mediated gene therapy reverses brain tumor-induced behavioral deficits. Mol. Ther. 16, 682–690.
King, G.D., Muhammad, A.K., Larocque, D., Kelson, K.R., Xiong, W., Liu, C., Sanderson, N.S., Kroeger, K.M., Castro, M.G., Lowenstein, P.R., 2011. Combined Flt3L/TK gene therapy induces immunological surveillance which mediates an immune response against a surrogate brain tumor neoantigen. Mol. Ther. 19, 1793–1801.
King, G.D., Rosene, D.L., Abraham, C.R., 2012. Promoter methylation and age-related downregulation of Klotho in rhesus monkey. Age 34, 1405–1419.
Ko, H.G., Jang, D.J., Son, J., Kwak, C., Choi, J.H., Ji, Y.H., Lee, Y.S., Son, H., Kaang, B.K., 2009. Effect of ablated hippocampal neurogenesis on the formation and extinction of contextual fear memory. Mol. Brain 2, 1.
Kunert, S.K., Hartmann, H., Haffner, D., Leifheit-Nestler, M., 2017. Klotho and fibroblast growth factor 23 in cerebrospinal fluid in children. J. Bone Miner. Metab. 35, 215–226.
Kuro-o, M., Matsumura, Y., Aizawa, H., Kawaguchi, H., Suga, T., Utsugi, T., Ohyama, Y., Kurabayashi, M., Kaname, T., Kume, E., Iwasaki, H., Iida, A., Shiraki-Iida, T., Nishikawa, S., Nagai, R., Nabeshima, Y.I., 1997. Mutation of the mouse klotho gene leads to a syndrome resembling ageing. Nature 390, 45–51.
Kurosu, H., Ogawa, Y., Miyoshi, M., Yamamoto, M., Nandi, A., Rosenblatt, K.P., Baum, M.G., Schiavi, S., Hu, M.C., Moe, O.W., Kuro-o, M., 2006. Regulation of fibroblast growth factor-23 signaling by klotho. J. Biol. Chem. 281, 6120–6123.
Kurosu, H., Yamamoto, M., Clark, J.D., Pastor, J.V., Nandi, A., Gurnani, P., McGuinness, O.P., Chikuda, H., Yamaguchi, M., Kawaguchi, H., Shimomura, I., Takayama, Y., Herz, J., Kahn, C.R., Rosenblatt, K.P., Kuro-o, M., 2005. Suppression of aging in mice by the hormone Klotho. Science 309, 1829–1833.
Lagace, D.C., Fischer, S.J., Eisch, A.J., 2007. Gender and endogenous levels of estradiol do not influence adult hippocampal neurogenesis in mice. Hippocampus 17, 175–180.
Li, G., Pleasure, S.J., 2005. Morphogenesis of the dentate gyrus: what we are learning from mouse mutants. Dev. Neurosci. 27, 93–99.
Li, G., Pleasure, S.J., 2014. The development of hippocampal cellular assemblies. Wiley Interdiscip. Rev. Dev. Biol. 3, 165–177.
Li, Q., Vo, H.T., Wang, J., Fox-Quick, S., Dobrunz, L.E., King, G.D., 2017. Klotho regulates CA1 hippocampal synaptic plasticity. Neuroscience 347, 123–133.
Li, S.A., Watanabe, M., Yamada, H., Nagai, A., Kinuta, M., Takei, K., 2004. Immunohistochemical localization of Klotho protein in brain, kidney, and reproductive organs of mice. Cell Struct. Funct. 29, 91–99.
Liu, H., Fergusson, M.M., Castilho, R.M., Liu, J., Cao, L., Chen, J., Malide, D., Rovira, I.I., Schimel, D., Kuo, C.J., Gutkind, J.S., Hwang, P.M., Finkel, T., 2007. Augmented Wnt signaling in a mammalian model of accelerated aging. Science 317, 803–806.
Logan, T.T., Rusnak, M., Symes, A.J., 2015. Runx1 promotes proliferation and neuronal differentiation in adult mouse neurosphere cultures. Stem Cell Res. 15, 554–564.
Maltare, A., Nietz, A.K., Laszczyk, A.M., Dunn, T.S., Ballestas, M.E., Accavitti-Loper, M.A., King, G.D., 2014. Development and characterization of monoclonal antibodies to detect klotho. Monoclon. Antib. Immunodiagn. Immunother. 33, 420–427.
Maren, S., Phan, K.L., Liberzon, I., 2013. The contextual brain: implications for fear conditioning, extinction and psychopathology. Nat. Rev. Neurosci. 14, 417–428.
Marin-Burgin, A., Schinder, A.F., 2012. Requirement of adult-born neurons for hippocampus-dependent learning. Behav. Brain Res. 227, 391–399.
Masso, A., Sanchez, A., Gimenez-Llort, L., Lizcano, J.M., Cañete, M., García, B., Torres-Lista, V., Puig, M., Bosch, A., Chillon, M., 2015. Secreted and transmembrane alphaKlotho Isoforms have different Spatio-Temporal profiles in the brain during aging and Alzheimer's disease progression. PLoS One 10, e0143623.
Mignone, J.L., Kukekov, V., Chiang, A.S., Steindler, D., Enikolopov, G., 2004. Neural stem and progenitor cells in nestin-GFP transgenic mice. J. Comp. Neurol. 469, 311–324.
Nacher, J., McEwen, B.S., 2006. The role of N-methyl-D-asparate receptors in neurogenesis. Hippocampus 16, 267–270.
Nacher, J., Varea, E., Miguel Blasco-Ibáñez, J., Gómez-Climent, M.A., Castillo-Gómez, E., Crespo, C., Martínez-Guijarro, F.J., McEwen, B.S., 2007. N-methyl-d-aspartate receptor expression during adult neurogenesis in the rat dentate gyrus. Neuroscience 144, 855–864.
Nagai, T., Yamada, K., Kim, H.C., Kim, Y.S., Noda, Y., Imura, A., Nabeshima, Y., Nabeshima, T., 2003. Cognition impairment in the genetic model of aging klotho gene mutant mice: a role of oxidative stress. FASEB J. 17, 50–52.
Nicola, Z., Fabel, K., Kempermann, G., 2015. Development of the adult neurogenic niche in the hippocampus of mice. Front. Neuroanat. 9, 53.
Okamoto, M., Inoue, K., Iwamura, H., Terashima, K., Soya, H., Asashima, M., Kuwabara, T., 2011. Reduction in paracrine Wnt3 factors during aging causes impaired adult neurogenesis. FASEB J. 25, 3570–3582.
Olariu, A., Cleaver, K.M., Cameron, H.A., 2007. Decreased neurogenesis in aged rats results from loss of granule cell precursors without lengthening of the cell cycle. J. Comp. Neurol. 501, 659–667.
Overstreet, L.S., Hentges, S.T., Bumaschny, V.F., de Souza, F.S., Smart, J.L., Santangelo, A.M., Low, M.J., Westbrook, G.L., Rubinstein, M., 2004. A transgenic marker for newly born granule cells in dentate gyrus. J. Neurosci. 24, 3251–3259.
Pastrana, E., Silva-Vargas, V., Doetsch, F., 2011. Eyes wide open: a critical review of sphere-formation as an assay for stem cells. Cell Stem Cell 8, 486–498.
Picano, E., Bruno, R.M., Ferrari, G.F., Bonuccelli, U., 2014. Cognitive impairment and cardiovascular disease: so near, so far. Int. J. Cardiol. 175, 21–29.
Piccin, D., Morshead, C.M., 2011. Wnt signaling regulates symmetry of division of neural stem cells in the adult brain and in response to injury. Stem Cell 29, 528–538.
Plumpe, T., Ehninger, D., Steiner, B., Klempin, F., Jessberger, S., Brandt, M., Römer, B., Rodriguez, G.R., Kronenberg, G., Kempermann, G., 2006. Variability of doublecortin-associated dendrite maturation in adult hippocampal neurogenesis is independent of the regulation of precursor cell proliferation. BMC Neurosci. 7, 77.
Pugh, P., Adlaf, E., Zhao, C.S., Markwardt, S., Gavin, C., Wadiche, J., Overstreet-Wadiche, L., 2011. Enhanced integration of newborn neurons after neonatal insults. Front Neurosci. 5, 45.
Qu, Q., Sun, G., Murai, K., Ye, P., Li, W., Asuelime, G., Cheung, Y.T., Shi, Y., 2013. Wnt7a regulates multiple steps of neurogenesis. Mol. Cell. Biol. 33, 2551–2559.
Rao, M.S., Hattiangady, B., Abdel-Rahman, A., Stanley, D.P., Shetty, A.K., 2005. Newly born cells in the ageing dentate gyrus display normal migration, survival and neuronal fate choice but endure retarded early maturation. Eur. J. Neurosci. 21, 464–476.
Rao, M.S., Hattiangady, B., Shetty, A.K., 2006. The window and mechanisms of major age-related decline in the production of new neurons within the dentate gyrus of the hippocampus. Aging Cell 5, 545–558.
Rao, M.S., Shetty, A.K., 2004. Efficacy of doublecortin as a marker to analyse the absolute number and dendritic growth of newly generated neurons in the adult dentate gyrus. Eur. J. Neurosci. 19, 234–246.
Reynolds, B.A., Rietze, R.L., 2005. Neural stem cells and neurospheres–re-evaluating the relationship. Nat. Methods 2, 333–336.
Sato, I., Miyado, M., Sunohara, M., 2005. NADH dehydrogenase activity and expression of mRNA of complex I (ND1, 51kDa, and 75kDa) in heart mitochondria of klotho mouse. Okajimas Folia Anat. Jpn. 82, 49–56.
Saxe, M.D., Battaglia, F., Wang, J.W., Malleret, G., David, D.J., Monckton, J.E., Garcia, A.D., Sofroniew, M.V., Kandel, E.R., Santarelli, L., Hen, R., Drew, M.R., 2006. Ablation of hippocampal neurogenesis impairs contextual fear conditioning and synaptic plasticity in the dentate gyrus. Proc. Natl. Acad. Sci. U. S. A. 103, 17501–17506.
Semba, R.D., Moghekar, A.R., Hu, J., Sun, K., Turner, R., Ferrucci, L., O'Brien, R., 2014. Klotho in the cerebrospinal fluid of adults with and without Alzheimer's disease. Neurosci. Lett. 558, 37–40.
Shardell, M., Semba, R.D., Rosano, C., Kalyani, R.R., Bandinelli, S., Chia, C.W., Ferrucci, L., 2016. Plasma klotho and cognitive decline in older adults: findings from the InCHIANTI study. J. Gerontol. Ser. A Biol. Sci. Med. Sci. 71, 677–682.
Shiozaki, M., Yoshimura, K., Shibata, M., Koike, M., Matsuura, N., Uchiyama, Y., Gotow, T., 2008. Morphological and biochemical signs of age-related neurodegenerative changes in klotho mutant mice. Neuroscience 152, 924–941.
Shipton, O.A., Paulsen, O., 2014. GluN2A and GluN2B subunit-containing NMDA receptors in hippocampal plasticity. Philos. Trans. R. Soc. Lond. Ser. B Biol. Sci. 369, 20130163.
Shiraki-Iida, T., Aizawa, H., Matsumura, Y., Sekine, S., Iida, A., Anazawa, H., Nagai, R., Kuro-o, M., Nabeshima, Y., 1998. Structure of the mouse klotho gene and its two transcripts encoding membrane and secreted protein. FEBS Lett. 424, 6–10.
Soule, J., Penke, Z., Kanhema, T., Alme, M.N., Laroche, S., Bramham, C.R., 2008. Object-place recognition learning triggers rapid induction of plasticity-related immediate early genes and synaptic proteins in the rat dentate gyrus. Neural. Plasticity 2008, 269097.
Stoll, E.A., Habibi, B.A., Mikheev, A.M., Lasiene, J., Massey, S.C., Swanson, K.R., Rostomily, R.C., Horner, P.J., 2011. Increased re-entry into cell cycle mitigates age-related neurogenic decline in the murine subventricular zone. Stem Cell 29, 2005–2017.
Suga, T., Kurabayashi, M., Sando, Y., Ohyama, Y., Maeno, T., Maeno, Y., Aizawa, H., Matsumura, Y., Kuwaki, T., Kuro-O, M., Nabeshima, Y., Nagai, R., 2000. Disruption of the klotho gene causes pulmonary emphysema in mice. Defect in maintenance of pulmonary integrity during postnatal life. Am. J. Respir. Cel. Mol. Biol. 22, 26–33.

Takeshita, K., Fujimori, T., Kurotaki, Y., Honjo, H., Tsujikawa, H., Yasui, K., Lee, J.K., Kamiya, K., Kitaichi, K., Yamamoto, K., Ito, M., Kondo, T., Iino, S., Inden, Y., Hirai, M., Murohara, T., Kodama, I., Nabeshima, Y., 2004. Sinoatrial node dysfunction and early unexpected death of mice with a defect of klotho gene expression. Circulation 109, 1776–1782.

Tang, Y.P., Shimizu, E., Dube, G.R., Rampon, C., Kerchner, G.A., Zhuo, M., Liu, G., Tsien, J.Z., 1999. Genetic enhancement of learning and memory in mice. Nature 401, 63–69.

Tsezou, A., Furuichi, T., Satra, M., Makrythanasis, P., Ikegawa, S., Malizos, K.N., 2008. Association of KLOTHO gene polymorphisms with knee osteoarthritis in Greek population. J. Orthop. Res. 26, 1466–1470.

Tsujikawa, H., Kurotaki, Y., Fujimori, T., Fukuda, K., Nabeshima, Y., 2003. Klotho, a gene related to a syndrome resembling human premature aging, functions in a negative regulatory circuit of vitamin D endocrine system. Mol. Endocrinol. 17, 2393–2403.

Wang, W., Pan, Y.W., Zou, J., Li, T., Abel, G.M., Palmiter, R.D., Storm, D.R., Xia, Z., 2014. Genetic activation of ERK5 MAP kinase enhances adult neurogenesis and extends hippocampus-dependent long-term memory. J. Neurosci. 34, 2130–2147.

West, M.J., Slomianka, L., Gundersen, H.J., 1991. Unbiased stereological estimation of the total number of neurons in thesubdivisions of the rat hippocampus using the optical fractionator. Anatomical Rec. 231, 482–497.

Wimmer, M.E., Hernandez, P.J., Blackwell, J., Abel, T., 2012. Aging impairs hippocampus-dependent long-term memory for object location in mice. Neurobiol. Aging 33, 2220–2224.

Yamazaki, Y., Imura, A., Urakawa, I., Shimada, T., Murakami, J., Aono, Y., Hasegawa, H., Yamashita, T., Nakatani, K., Saito, Y., Okamoto, N., Kurumatani, N., Namba, N., Kitaoka, T., Ozono, K., Sakai, T., Hataya, H., Ichikawa, S., Imel, E.A., Econs, M.J., Nabeshima, Y., 2010. Establishment of sandwich ELISA for soluble alpha-Klotho measurement: age-dependent change of soluble alpha-Klotho levels in healthy subjects. Biochem. Biophysical. Res. Commun. 398, 513–518.

Yokoyama, J.S., Sturm, V.E., Bonham, L.W., Klein, E., Arfanakis, K., Yu, L., Coppola, G., Kramer, J.H., Bennett, D.A., Miller, B.L., Dubal, D.B., 2015. Variation in longeivity gene KLOTHO is associated with greater cortical volumes. Ann. Clin. Translational. Neurol. 2, 215–230.

Yoshida, T., Fujimori, T., Nabeshima, Y., 2002. Mediation of unusually high concentrations of 1,25-dihydroxyvitamin D in homozygous klotho mutant mice by increased expression of renal 1alpha-hydroxylase gene. Endocrinology 143, 683–689.

Zeldich, E., Chen, C.D., Colvin, T.A., Bove-Fenderson, E.A., Liang, J., Tucker Zhou, T.B., Harris, D.A., Abraham, C.R., 2014. The neuroprotective effect of Klotho is mediated via regulation of members of the redox system. J. Biol. Chem. 289, 24700–24715.

Zeldich, E., Chen, C.D., Avila, R., Medicetty, S., Abraham, C.R., 2015. The anti-aging protein klotho enhances Remyelination following Cuprizone-induced Demyelination. J. Mol. Neurosci. 57, 185–196.

Zeng, C., Pan, F., Jones, L.A., Lim, M.M., Griffin, E.A., Sheline, Y.I., Mintun, M.A., Holtzman, D.M., Mach, R.H., 2010. Evaluation of 5-ethynyl-2'-deoxyuridine staining as a sensitive and reliable method for studying cell proliferation in the adult nervous system. Brain Res. 1319, 21–32.

Zhou, L., Li, Y., Zhou, D., Tan, R.J., Liu, Y., 2013. Loss of Klotho contributes to kidney injury by derepression of Wnt/beta-catenin signaling. J. Am. Soc. Nephrol. 24, 771–785.